THE JOURNAL OF PHYSICAL CHEMISTRY B
A JOURNAL OF THE AMERICAN CHEMICAL SOCIETY

pubs.acs.org/JPCB

Article

Subpicosecond Molecular Rearrangements Affect Local Electric Fields and Auto-Dissociation in Water

Stephen H. Garofalini* and Jesse Lentz

Cite This: J. Phys. Chem. B 2023, 127, 3392−3401

Read Online

ACCESS | Metrics & More | Article Recommendations | Supporting Information

ABSTRACT: Molecular simulations of auto-dissociation of water molecules in an 81,000 atom bulk water system show that the electric field variations caused by local bond length and angle variations enhance proton transfer within ~600 fs prior to auto-dissociation. In this paper, auto-dissociation relates to the initial separation of a proton from a water molecule to another, forming the $H^3{}_3O^+$ and OH^- ions. Only transfers for which a proton's initial nearest covalently bonded oxygen remained the same for at least 1 ps prior to the transfer and for which that proton's new nearest acceptor oxygen remained the same for at least 1 ps after the transfer were evaluated. Electric fields from solvent atoms within 6 Å of a transferring proton (H*) are dominant, with little contribution from farther molecules. However, exclusion of the accepting oxygen in such electric field calculations shows that the field on H* from the other solvent atoms weakens as the time to transfer becomes less than 600 fs, indicating the primary importance of the accepting oxygen on enabling auto-dissociation. All resultant OH^- and H_3O^+ ion pairs recombined at times greater than 1 ps after auto-dissociation. A concentration of 8.01×10^{17} cm^{-3} for these ion pairs was observed. The simulations indicate that transient auto-dissociation in water is more common than that inferred from dc-conductivity experiments (10^{-5} vs 10^{-7}) and is consistent with the results of calculations that include nuclear quantum effects. The conductivity experiments require the rearrangement of farther water molecules to form hydrogen-bonded "water wires" that afford long-range and measurable proton transport away from the reaction site. Nonetheless, the relatively large number of picosecond-lived auto-dissociation products might be engineered within 2D layers and oriented external fields to offer new energy-related systems.

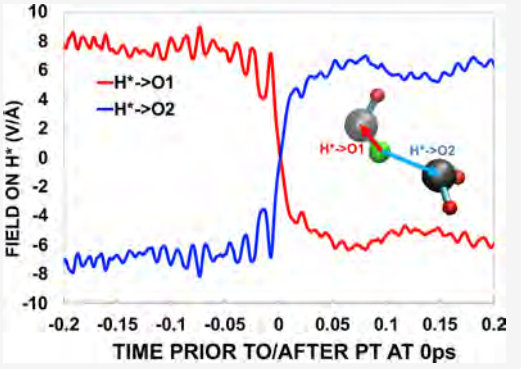

INTRODUCTION

The presence and migration of protons and hydroxide (OH^-) ions in water play an important role in physical, chemical, and biological applications and have attracted a large number of studies regarding the mechanisms of the transfer of protons in liquid water. However, a preponderance of these studies involved proton transfer from an existing hydronium ion H_3O^+ ion to an adjacent H_2O molecule[1−14] and subsequent long-range separation that is dependent on the existence of a hydrogen-bond chain; much of the work has been reviewed.[15] Many of these studies involved molecular computations that can provide information on the femtosecond to picosecond timeframes. Far fewer studies have been done regarding the initial formation of the H_3O^+ ion and OH^- ion in neat water via the auto-dissociation of a water molecule, as shown in reaction 1a.

$$2H_2O \rightarrow H_3O^+ + OH^- \quad (1a)$$

One reason for this is the understanding that the formation of these ions in water is a rare event based on electrochemical studies used to extrapolate their low concentrations in pure water and by equilibrium thermodynamics.[16−18] However, for experimental measurement of the product ions, long-distance structural migration of the ions requires formation of hydrogen-bonded chains for a Grotthuss-like mechanism of proton transport away from the reaction site. Hassanali et al. discussed the required compression of the H-bond wire to enable such proton migration via structural diffusion.[9] Such long-range solvent rearrangement would be expected to raise the barrier for migration and capture of the charged species in electrochemical measurements. Without the formation of such a path, rapid neutralization of the product ions occurs, potentially leading to the low concentration of measurable species.

In the work presented in this current paper, we only discuss the formation of the product ions that last at least 1 ps, without regard to farther separation of these ions and apply the term auto-dissociation to this initial formation of product ions and associated electric fields. This would be different from other

Received: September 11, 2022
Revised: March 30, 2023
Published: April 10, 2023

works that use the term auto-dissociation to include the stabilization of the separated ions.

In ab initio calculations of a small system of 32 molecules, Trout and Parrinello showed the free energy barrier for auto-dissociation below 10 kcal/mol and a barrier above 15 kcal/mol for separation of the product ions using a distance constraint model.[19] Sprik used constraints on the number of protons on donating and accepting species that separate the ions with a similar high barrier.[20] Moqadam et al. added additional constraints in their calculations of auto-dissociation that also included separation of the ions.[21] Geissler et al. similarly considered stabilization that required separation of the ion pairs in their calculations.[22] Equilibrium thermodynamics indicates a free energy barrier of near 20 kcal/mole. A high barrier for product-ion separation would coincide with a low concentration of measurable species. Others employing the term auto-dissociation of the water molecule have included this subsequent migration of the product ions away from the reaction site as a part of auto-dissociation, with similarly high barriers.[23,24]

While the concentration of currently "measurable" ion product species and required stabilization (separation) of these species are relevant, that is not the topic of the current paper. A question that arises is: "Can these relatively short-lived species be gatherable?"

Geissler et al. acknowledged the "existence of many short-lived hydronium and hydroxide ions in water" whose lifetime is less than 100 fs.[22] Additional work also obtained data that indicated the presence of many of these short-lived transient ions in water.[23,25−28] Time-resolved spectroscopies may miss these short-lived events because of the predominance of the role of intact water molecules on the output spectrum. In our work, we will show that there is a larger number of product ions lasting longer than 100 fs that are consistent with ab initio calculations that include nuclear quantum effects (NQEs).[29] In their ab initio calculations, Ceriotti et al. showed that inclusion of NQEs brings about a concentration of 10^{-3} auto-dissociation events. As will be shown below with regard to the work presented in the current paper, we similarly observed such a concentration of auto-dissociation events that last for at least 1 ps prior to neutralization.

Neutralization of these product ions occurs via eq 1b.

$$H_3O^+ + OH^- \rightarrow 2H_2O \quad (1b)$$

Neutralization often occurs rapidly (within femtoseconds), preventing formation of experimentally measurable ions that require long-lived separation of the ions.[9,11,22,27,30,31] Following an auto-dissociation event, rapid neutralizations can infrequently be prevented by the structural diffusion of the H_3O^+ complex or the OH^- complex away from the reaction site that has been well documented.[5,8,9,11,12,22,30,32−34] Such behavior is shown in reactions 1c and 1d.

$$H_3O^+ + H_2O \rightarrow H_2O + H_3O^+ \quad (1c)$$

$$OH^- + H_2O \rightarrow H_2O + OH^- \quad (1d)$$

However, using a polarizable water potential, Bai showed that even by removing a proton from their water and placing it far from the formed OH^- ion, neutralization was observed in the 3D system.[31] However, they did not determine the electric fields on the ions caused by solvent species.

The electric field from neighboring atoms is known to play an important role in affecting auto-dissociation as well as subsequent longer-ranged proton transfer that is dependent on the presence of the hydrogen-bond chain along which the transferring proton moves.[22,35−38] As mentioned, computational simulations offer a method for evaluating subpicosecond proton behavior in water. However, reactions 1a−1d would be unavailable in those molecular simulations that employ certain popular water potentials that describe rigid and nondissociable water molecules. Nonetheless, simulations employing such potentials have been used to determine the electric field imposed on the proton in a water molecule from other atoms and the implications of such a field have been related to the possibility for auto-dissociation.[35−38] Electric fields on a proton caused by neighbor atoms varied from 2 to 3.5 V/Å depending on the hydrogen bond length,[36,38] with the higher fields at shorter lengths. However, auto-dissociation via proton transfer would not actually occur in such calculations using non-dissociable water potentials although the values of the observed fields are important.

Application of ab initio calculations to auto-dissociation of the water molecule has provided useful data regarding electric fields on a proton in general and the implications on proton transfer via eq 1a.[9,11,19,22,29,39,40] For example, Hermansson and Ojamäe showed that an applied electric field of ∼3 V/Å on a configuration of only two H_2O molecules was sufficient to remove the proton-transfer barrier to allow for reaction 1a.[39] Geissler et al. used a system of 32 water molecules to show auto-dissociation and the necessary structures for separation of the resulting ions.[22] Saitta et al. used a system of 64 molecules and showed that an external applied electric field of only 0.3−0.6 V/Å was sufficient to enhance dissociation.[40] This small external field would be in addition to the local fields caused by solvent molecules.

These various classical and ab initio studies provide a useful understanding of the role of local electric fields on auto-dissociation and proton transfer. Since it was shown that an electric field of ∼3 V/Å is all that is required to allow for proton transfer from a donor water molecule to an acceptor water molecule,[39] if such a local electric field caused by the solvent molecules is sufficiently strong, then only a slight external enhancement, as shown by Saitta et al.,[40] is sufficient to significantly enhance auto-dissociation.

In order to evaluate the solvent-generated electric fields on protons that are actually able to transfer during auto-dissociation of H_2O molecules in liquid water in molecular dynamics simulations involving large numbers of molecules, a reactive interatomic potential that allows for dissociation of the water molecule to form the ions shown in eq 1a is employed. Of course, the neutralization (1b) and structural diffusion of the ions (1c and 1d) are also available with such a potential, some of which has been previously reported.[10,41] The advantage of using such a reactive interatomic potential is that large systems can be studied and no prior assumptions regarding which protons transfer need to be made. Similarly, no extraneous additions on a common rigid molecule interaction potential or atomistic configuration need to be made to enable dissociation. This work also acts as another test of the viability of the potential to reproduce another property of water that was not within the original design parameters.[42]

Results show that local electric fields on transferring protons have values consistent with previous data but also show the important relation between field strength and angular rotations toward the accepting molecule on transfer. Another important finding that relates to femtosecond rattling versus longer-lived

https://doi.org/10.1021/acs.jpcb.2c06490
J. Phys. Chem. B 2023, 127, 3392−3401

proton transfer is the role of the orientation of the accepting molecule on the stability of the transferred proton. Such a relation may be related to electron localization functions (ELFs) of reacting water molecules. While the ions that lasted at least 1 ps as products of the auto-dissociation events are presented in detail here, all such newly formed ions eventually neutralized at times greater than 1 ps after auto-dissociation. In addition, a significant number of shorter-lived (<1 ps) ion pairs also occurred. The rapid neutralization of the ions in the current study would be consistent with the low concentration of measurable ions observed in dc conductivity experiments. The latter experiments require the formation of hydrogen-bonded "wires" along which subsequent proton transfers migrate the ion complexes away from the reaction site. Nonetheless, the results of the current simulations show that auto-dissociation (as defined in this paper) is not uncommon in water. Such a finding is similar to conclusions of ab initio calculations referenced above, but with significantly larger system size and more dissociation events, and to interpretations of electrodynamic and IR data.[25,27,28]

METHODS: COMPUTATIONAL PROCEDURE

The molecular dynamics simulations use a reactive, all-atom potential with two- and three-body terms that allows for dissociation of water molecules.[42] It has been shown to reproduce a variety of bulk water properties such as the structure, heat of vaporization (10.5 kcal/mol), diffusion coefficient (2.4×10^{-5} cm^2/s), and frequency spectrum.[42,43] Hydrogen-bond lifetimes in bulk water (2.1 ps) are consistent with experimental data.[41] Mechanisms of proton transport in bulk water via inserted H_3O^+ ions[10,41] and large jump angular correlation functions are consistent with experiment.[41] The free energy barrier to proton transfer from a hydronium ion to an adjacent water molecule in bulk water at an O−O spacing of 2.4 Å of 0.8 kcal/mol[10] is observed with this potential, close to the ab initio value of 0.6 kcal/mol[44] using a classical proton. The decrease in the O−O spacing between reacting species results in a decrease in the barrier to proton transfer, especially for distances below 2.5 Å. The frequency−frequency correlation function observed in simulations with this potential showed short-time correlations similar to the experiment and long-time behavior that coincides with the O−O vibrations. Interfacial behavior observed with this potential shows reactions on silica surfaces forming surface silanols (SiOHs) at concentrations (4−5 nm^{-2}) consistent with the experiment,[34] migration of protons at the silica surface via surface silanols and adjacent waters, forming H_3O^+ ions,[33,34,43] consistent with ab initio calculations,[45] free energy barriers to hydroxylation of silica exposed to water that fit within experimental data[46] (15 kcal/mol vs 14−24 kcal/mol from the experiment and 18−39 kcal/mol from ab initio calculations), the high thermal expansion of nanoconfined water that reproduces experimental data and provides an explanation for the increased expansion,[47,48] and diffusion of water through nanoporous silica.[49] These results indicate a high level of transferability to different scenarios.

The large bulk water system used in this work was described previously.[41] The system was initialized with 27,000 water molecules and run with periodic boundaries in all dimensions at a constant number, temperature, and pressure (NPT), with a temperature of 298 K and a pressure of 1 atm, for 200 ps. The system size was 96.509 Å × 92.582 Å × 89.477 Å in the x, y, and z dimensions, respectively. An integration timestep of 0.1 fs was used for all runs. Following this equilibration, a 100 ps production run was performed at constant NPT; all data were obtained from this production run. Configurations from the production run were saved every 1 fs, resulting in 10^5 saves. Three hydronium/hydroxide pairs formed during the 200 ps equilibration run and were therefore present at the beginning of the production run but were not considered in the current analysis. As previously shown, the lifetime autocorrelation functions of the ions using this potential[10] follow the multiexponential decay observed by others.[50−52]

The local electric field at the position of a proton was calculated by taking a vector sum of the individual Coulomb forces from all oxygen and hydrogen ions within specific cutoff radii (r_c), 6 and 15 Å. Electric fields from specific atoms or groups of atoms were also calculated, as shown below. As per the potential, hydrogen ions have a point charge of +0.452e and oxygen ions have a point charge of −0.904e, where e is the elementary charge. The following expression was used to calculate the electric field vector on atom i, where $k = \frac{1}{4\pi\varepsilon_0}$ is Coulomb's constant, q_j is the charge of atom j, r_{ji} is the separation distance between atoms j and i, and $\hat{r}_{ji}$ is a unit vector pointing in the direction from atom j toward atom i.

$$\vec{E}_i = k\sum_{j\neq i}^{r<r_c} \frac{q_j}{r_{ji}^2}\hat{r}_{ji} \tag{2}$$

The field is represented by projecting this field vector onto one of the several directions: the direction pointing from the proton toward its original donor oxygen (O1), the direction pointing from the proton's original acceptor oxygen (O2) toward the proton, and the direction pointing from O2 toward O1. The projection of the field on any of these directions (corresponding to unit vector $\hat{r}_d$), is given by $E_{i,d} = \vec{E}_i \cdot \hat{r}_d$.

Throughout the 100 ps production run, a proton transfer is defined as an event where the proton's nearest oxygen changes between two consecutive configurations. We analyze only the subset of proton transfers for which the proton's initial nearest covalently bonded oxygen (O1) remained the same for at least 1 ps prior to the transfer and for which the proton's new nearest oxygen (O2) remained the same for at least 1 ps after the transfer, forming a covalent bond to O2. O1 and O2 are therefore the donor and acceptor oxygens, respectively, during a transfer. This criterion eliminates transfers that involve extremely short-time (femtoseconds) rattling due to large vibrational amplitudes and includes only those with a well-defined time of transfer (t_0) that allows electric fields to be plotted as a function of time relative to t_0. The 100 ps trajectory contained 20 transfers meeting this criterion as autoionization reactions (eq 1a). However, all these transfers eventually neutralized via eq 1b at times greater than 1 ps on the acceptor oxygen. We also include information regarding the other shorter-lived ions that last in the sub-picosecond range in order to determine the concentration of ions in our simulated system. These additional data provide an indication of the relationship between the concentration of ions seen in our work and the values predicted by Artemov and colleagues.[25,27,28]

RESULTS AND DISCUSSION

There are multiple ways to evaluate the local electric field on the transferring proton, H*, prior to and post auto-dissociation

https://doi.org/10.1021/acs.jpcb.2c06490
J. Phys. Chem. B 2023, 127, 3392−3401

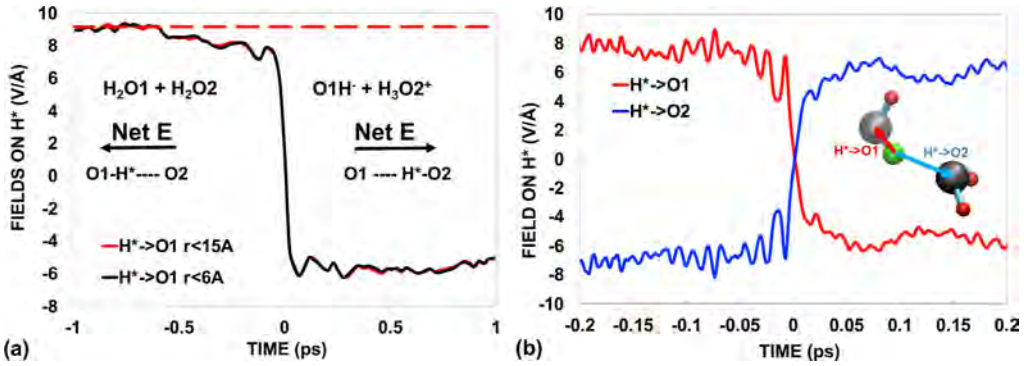

Figure 1. (a) Average local e-field on H* as a function of time from 1 ps prior to PT (labeled−1) to 1 ps after PT from all atoms within 15 Å and within 6 Å of H*. The dashed line is the average value of the field on all protons in the system and is not time-dependent. (b) Higher resolution over times within 0.2 ps of PT showing oscillations in the local e-field. The inset shows H* to O1 and H* to O2 directions.

of a water molecule. One way is to look at the total field on H* from all atoms within specific distances of H*; another is to look at the intermolecular electric field on H* from atoms excluding those on the donating molecule (the one that shows auto-dissociation); a third is to look at the fields from specific neighbor atoms to H*. All three will be shown below for the condition in which the transferring proton, H*, existed on O1 (the oxygen in the donating water molecule) for greater than 1 ps prior to proton transfer (PT) and remained on O2 (the accepting oxygen) for at least 1 ps after PT.

Figure 1a shows the average electric fields on H* in those water molecules that showed the proton transferring during auto-dissociation for the given times. The e-fields include all atoms within 15 Å of H* as well as all atoms within only 6 Å of H*. The label "H*− > O1" denotes the field oriented along the H* to O1 direction; it is positive prior to proton transfer and becomes negative after PT, showing the important effect on the direction of the e-field that is created by the oxygen to which H* is bonded. Results show that the electric field on H* is dominated by those atoms within 6 Å of H* and atoms farther away have little to no effect. Such a result is consistent with calculations by Reischl et al.[35] who used a cutoff of 7 Å and others regarding the importance of local structure on these electric fields.[19,37,38] Another feature is the change in slope of the H*−O1 e-field line occurring near −0.6 ps, as will be discussed below. The dashed line indicates the electric fields averaged over all nontransferring protons in the system along their H to O1 direction and does not have an actual time constraint.

Figure 1b provides higher resolution and more data points of the e-fields at times closer to PT (±200 fs), showing an increase in the amplitude of the oscillations within the last ∼50 fs (−0.05 ps) prior to PT. The label "H*− > O2" is the field along the H* to O2 direction, as shown in the inset, and the oscillations are nearly a mirror image of the H* to O1 data. Note that the strength of the e-field in the H*−O2 direction post transfer is less positive than the field in the H*−O1 direction prior to PT. This is because H* is on an H_3O^+ ion post transfer and the other two protons on O2 create a repulsive field on H*. This would enhance the eventual transfer of one of the protons on O2 that relates to the lifetime of H_3O^+ ions that is in the 2 ps range. Additional details showing the e-fields on the individual H* to O1 are given in Supporting Information, Figure S1 in 1 fs increments over 100,000 fs, including the average and standard deviation.

Figure 2 provides additional information regarding the cause of the e-field oscillations shown in Figure 1b. The average H*−

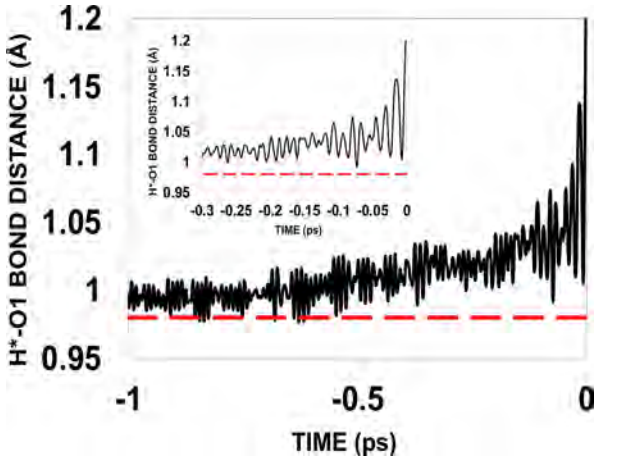

Figure 2. Average H* to O1 covalent bond length as a function of time prior to auto-dissociation at 0 ps showing an increase in the length within ∼0.6 ps of PT. The inset shows increased covalent bond length oscillations as the time approaches PT. The dashed line is average covalent bond length for all protons (0.98 Å).

O1 covalent bond length as a function of time is shown in Figure 2. This length increases near 0.6 ps prior to PT (−0.6 ps), a time that is similar to the time of the slope change occurring in Figure 1a. The inset shows that the bond length oscillations become larger in the final 300 fs prior to proton transfer at 0 ps. The covalent bond lengths for the H* are longer than the covalent bond length averaged over all protons in the system that is shown by the dashed line (which is not associated with the time axis).

An example of an auto-dissociation reaction is shown in Figure 3a−c, in which the two relevant waters (circled, with H* in green and O1 and O2 in gray) may be relatively separated in (a), approach from (a) to (b), with H* transferring to O2 in (c).

Figure 4 shows the O2−O1−H* angle averaged over all H* in the 1 ps prior to transfer. Similar to Figures 1a and 2, a change in the slope of these angles occurs near −0.6 ps. A couple pairs had higher starting O2−O1−H* angles. One of these high-angle reacting pairs is shown in Figure 5, where the starting angle is 137°. Nonetheless, the donating water rotates toward O2 and the transfer occurs. While other reacting

https://doi.org/10.1021/acs.jpcb.2c06490
J. Phys. Chem. B 2023, 127, 3392−3401

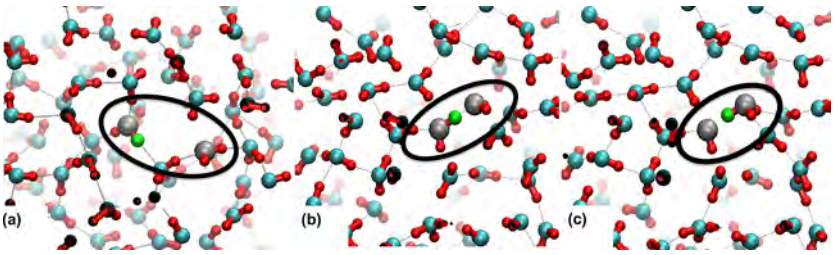

Figure 3. Snapshots of an auto-dissociation forming OH^- and H_3O^+ as a function of time from (a) to (c) for the molecules circled, with H* in green and O1 and O2 in gray (other O in cyan and H in red).

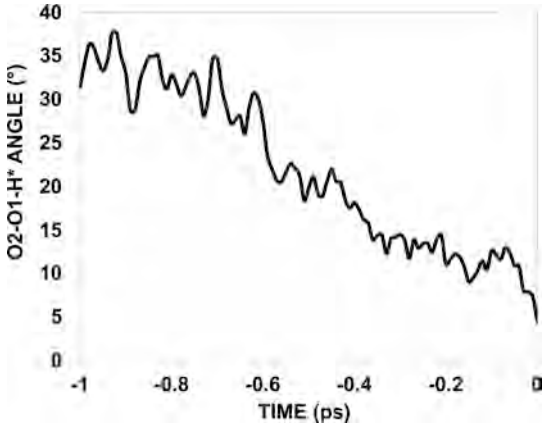

Figure 4. O2−O1−H* average angle distribution for times before proton transfer from −1 to 0 ps.

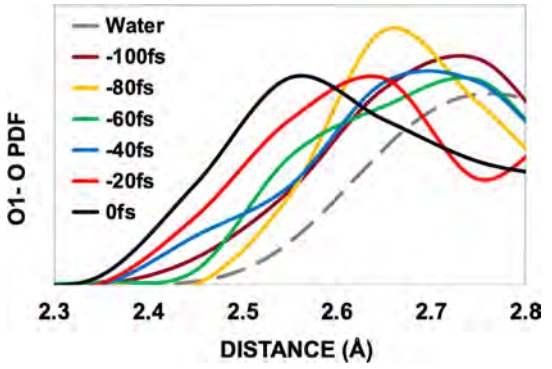

Figure 6. Pair distribution function (PDF) of O1 to all other O for times just prior to PT (at 0 fs), with comparison to bulk water O−O PDF showing a significant decrease in the first neighbor (O2) distance. Smaller O1−O2 distances have been shown to significantly decrease the barrier to PT.

molecule pairs have low starting O2−O1−H* angles at −1 ps, such large angle outliers are nonetheless important because they show that the proton transfer does not need H* to be oriented toward O2 for a significant amount of time in order for a transfer to occur.

However, this large rotation may impart a kinetic effect of bringing the reacting molecules closer together. This is relevant in that an important feature in PT is related to the O1−O2 distance just prior to PT, as shown in Figure 6. As time approaches PT at 0 fs, the O1 to first neighbor O (O2) distance decreases significantly in comparison to O−O spacing in bulk water (also shown). Molecular simulations and ab initio calculations have shown that decreased O−O spacing significantly lowers the barrier to proton transfer.[10,44,53] While those previous studies related to H_3O^+ ions, O1−O2 spacing plays an important role in enabling PT between water molecules[31,41] and is consistent with the increased H*−O1 distance shown in Figure 2 that decreases the H* to O1 bond strength and similarly enhances PT. A similar conclusion was presented by Ceriotti et al. regarding the importance of the O−O spacing on proton transfer when including NQE.[29]

Figure 5 also shows the two reacting molecules in a configuration with both oxygens aligned upward. Hassanali et al. showed a low barrier for proton transport in this alignment.[54] They also observed Voronoi volumes in the 4−7 $Å^3$ range around the donating oxygen. Table 1 shows the average Voronoi volumes around the H*, O1, and O2 atoms at the time of proton transfer, with comparison to the average value obtained for each species averaged over 100 config-

Table 1

	H*	O1	O2	500 oxygens	500 hydrogens
average vol 100 ps	11.754	6.341	6.337	6.369	11.658
average vol at PT	9.124	5.723	5.272		

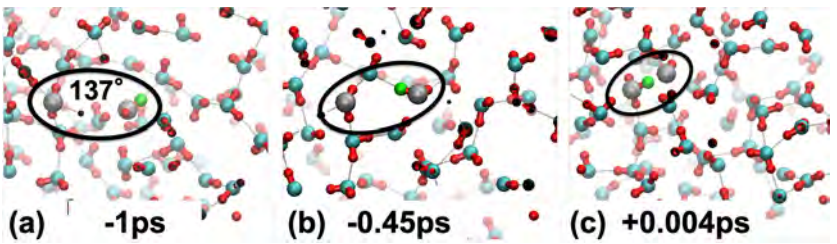

Figure 5. Snapshots of an auto-dissociation reaction starting from a large O2−O1−H* angle (137°) in (a), forming OH^- and H_3O^+ as a function of time from (a) to (c) for the molecules circled, with H* in green and O1 and O2 in gray. Note the rotation to the small angle in (b).

https://doi.org/10.1021/acs.jpcb.2c06490
J. Phys. Chem. B 2023, 127, 3392−3401

urations spaced over the 100 ps run for 500 random oxygens and 500 random hydrogens.

Several items can be observed in Table 1: (1) the average Voronoi volumes around H*, O1, and O2 over 100 ps are similar to the average of 500 random H's and O's over 100 ps; (2) the Voronoi volumes around the donating and accepting oxygens at the time of PT are similar to the values presented by Hassanali et al. in their ab initio calculations; and (3) there is a ∼10−20% decrease in the volumes around H*, O1, and O2 at the time of PT in comparison to the average for H and O in the system.

A recurring theme in Figures 1a, 2, and 4 is the change in slope of the data starting around −0.6 ps in each figure. The orientation of the molecules affects the e-fields on H* toward O1 and O2 and the H*−O1 bond length oscillations just prior to proton transfer.

The e-fields on H* can be delineated by including only specific neighbors, as shown in the next several figures. Figure 7 shows the contributions to the field on H* in the H* to O1

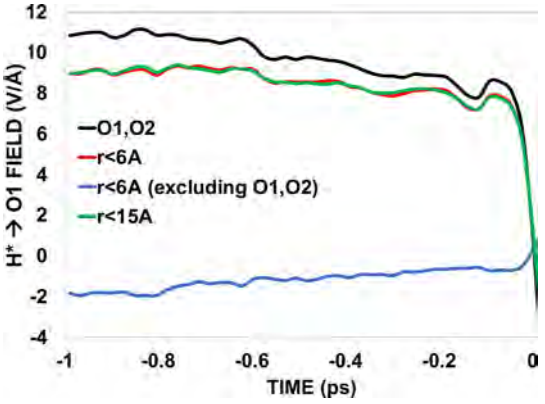

Figure 7. E-fields on H* in the H* to O1 direction from different sets of neighboring atoms showing the important effect of oxygens O1 and O2 on the field and the weakening of the e-field created by neighboring atoms excluding O1 and O2. See text.

direction from just the donating and accepting oxygen atoms, O1 and O2 (labeled "O1 and O2"), all atoms within 6 Å of H* (labeled r < 6 Å), with and without the inclusion of O1 and O2, and all atoms within 15 Å of H* (labeled r < 15 Å). The net field is dominated by the fields from just the two closest oxygen atoms, O1 and O2. Being strongly positive indicates that O1 provides the dominant attractive e-field on H* prior to PT since this is plotted in the H* to O1 direction. The field in this direction weakens when time approaches 0 ps, indicating the importance of O2.

Based on our previous simulation data regarding covalent and hydrogen bond lengths for those molecules that showed PT (0.996 and 1.72 Å, respectively),[41] O1 contributes 13.1 V/Å attraction on H* at 0.996 and O2 counters this strong field with a value of −4.4 V/Å at 1.72 Å, partially cancelling the field from O1 in the H* to O1 direction. These distances are different from the average of all water molecules and relate only to those that showed PT[41] and are consistent with an increased covalent bond length coincident with a shorter hydrogen bond length.[41] These fields would give a net field of 8.7 V/Å if the O2−O1−H* angle was zero degrees. However, because this angle in not zero degrees, the net field from only the two oxygens, O1 and O2, in the H* to O1 direction near −1.0 ps is ∼11 V/Å. This is due to the initially larger average O2−O1−H* angle from −1 ps to approximately −0.6 ps that reduces the contribution from O2 on H* in the H*−O1 direction (see the inset in Figure 1b). As the angle decreases in time, the net e-field from O1 and O2 in the H* to O1 direction decreases as O2 makes a stronger contribution to offset that from O1 on H*. This e-field approaches ∼9 V/Å within 200 fs of PT as the O2−O1−H* angle drops to near 10° at this time, as shown in Figure 4. The e-field from all atoms (including O1 and O2) within a distance r < 6 Å and r < 15 Å from H* lower the total field to ∼9 V/Å at −1 ps, indicating that the neighbors counter the strong field from O1 and provide a net e-field of ∼−2 V/Å on H* in the H* to O1 direction that enhances proton transfer. Again, the atoms beyond 6 Å make little additional contribution to the e-field on H*. The importance of O1 and O2 on the net e-field on H* is also shown in Figure 7 with the field from all atoms within 6 Å of H*, excluding O1 and O2. It is clear that all other atoms place a negative e-field on H* in the H* to O1 direction prior to PT, thus weakening the H* to O1 bond and enhancing a transfer. However, and importantly, this negative solvent e-field on H* that excludes O1 and O2 decreases as time approaches PT (0 ps). This indicates that the solvent atoms excluding O1 and O2 create a lowered inducement for H* to transfer to O2. Evaluation of the e-field caused by the two protons on O2 showed that they create a positive ∼1.3 V/Å on H* in the H* to O1 direction at −1.0 ps but become more positive to ∼2.3 V/Å just prior to PT. This repulsion by these protons on O2 is a part of the cause of the decrease in the inducement to PT by solvent atoms on H* excluding O1 and O2. As shown next, this proton-generated field on H* is offset when O2 is included in the solvent calculations.

These results are corroborated by the data in Figure 8 that shows the intermolecular e-field on H* provided by all atoms

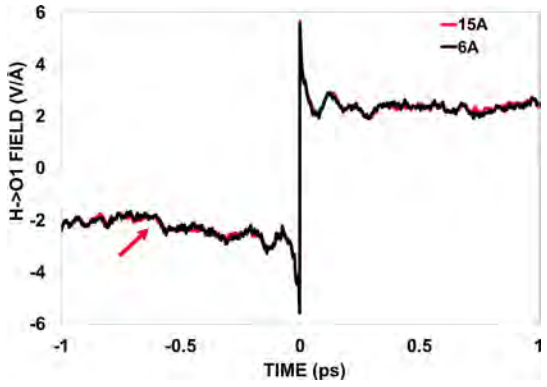

Figure 8. Intermolecular e-field on H* in the H* to O1 direction (excludes O1 and other H on O1) for atoms within 6 and 15 Å of H*. The arrow shows slope change near −0.6 ps again.

at r < 6 Å and similarly r < 15 Å, excluding O1 and the other proton on O1. The negative field in the H* to O1 direction indicates that these intermolecular fields lessen the e-field on H* to O1 and therefore enhance proton transfer from O1 to O2, consistent with the implications from Figure 7. As the O2−O1−H* angle decreases after ∼−0.6 ps shown in Figure 4, the arrow in Figure 8 indicates that a similar change occurs in which the e-field in the H* to O1 direction becomes more negative.

Figure 8 also provides two important features: one, the intermolecular e-field is ∼−2 V/Å at −1 ps and two, the

https://doi.org/10.1021/acs.jpcb.2c06490
J. Phys. Chem. B 2023, 127, 3392−3401

intermolecular e-field approaches −3.5 V/Å in the last 100 fs prior to PT (with a rapid change to ∼−5 V/Å at PT). The value of ∼−2 V/Å at −1 ps is slightly larger than that predicted by Reischl et al. who used a rigid molecule potential and calculated the field from the neighbors at the midpoint of the O1−H* bond.[35] (The midpoint location lessens the effect of O2 on the calculation because of the longer distance from O2 to the midpoint versus to H*.) Using a nonreactive SPC-type water model, Smith et al. found a value near −2 V/Å on H with a hydrogen-bond length near 1.8 Å, increasing to −3.5 V/Å with decreasing H-bond length.[36] With the increasing covalent O1− H* bond length shown in Figure 2, there is a concurrent decrease in the hydrogen bond length between H* and O2, the accepting oxygen, as shown previously,[41] which causes a weakening of the bond of H* to O1. This decrease in the hydrogen bond length and the −3.5 V/Å e-field value seen in the current data would be consistent with previous data.[36] Of course, those simulations using nonreactive potentials did not show the e-fields at the time of auto-dissociation or the changes in the e-field as the covalent OH bond elongates and the proton transfers, as shown here.

Previous analysis of the ELF of a dimer water molecule or a water molecule in water showed that the lone-pair electrons around the water molecule play an important role in the formation of the hydrogen bond.[19,32] In the current work shown here using the multibody potential, the simulations inherently reproduce this effect and show that in addition to the local electric field from solvent atoms that plays an important role in proton transfer, the final stability of the transferred proton also depends on the orientation of the accepting molecule to enable a proton transfer that lasts at least 1 ps on the accepting molecule. This behavior is manifested in the formation of very short-lived (fs) ions because of the misorientation of the receiving water molecule as discussed in the Supporting Information and Figures S2 and S3.

Volkov and Artemov provided a concentration of 5.4×10^{20} cm^{-3} ion pairs deduced from their studies,[25] although they state that the data should be considered as "estimates". Analysis of the cumulative concentration of long-lived (>1 ps) ion pairs in our data discussed above (per the 100 ps runtime) results in a concentration of 8.01×10^{17} cm^{-3} (1.33×10^{-3} mol/L). This is considerably less than the Volkov result but still 2 orders of magnitude higher than that expected from dc conductivity data (10^{-5} vs 10^{-7}). Inclusion of the shorter-lived ion pairs increases the cumulative concentration of ion pairs as a function of the time at which we start the cumulation, as shown in Figure 9. Of course, the shortest femtosecond lifetimes would be considered rattling. The average lifetime for those lasting more than 1ps was 2.5ps.

Ceriotti et al. showed the effect of including NQEs in ab initio calculations of hydrogen-bond fluctuations and proton transfer.[29] With inclusion of NQE in the calculations, they observed protons on the order of 10^{-3} in the structural region that corresponds to auto-dissociation. They also associate these fluctuations to a decrease in the O−O spacing, similar to what we and others have shown. It is clearly surprising (and perhaps fortuitous) that we observe 20 1 ps-lived auto-dissociations out of 27,000 waters (∼10^{-3}). In their ab initio calculations, Moqadam et al. also found that with local order parameters in their ideal range, dissociation increased from 10^{-7} to 0.4.[21]

Finally, as mentioned above, all 20 transferring protons via eq 1a eventually returned to their original donating oxygen within the 100 ps analysis timeframe of the simulations via eq 1b. The resulting H_3O^+ and OH^- ions created during auto-dissociation had e-fields on the transferred proton that reduced the stability of these ions during the simulations. Using a new starting time for the proton, labeled H** on the H_3O^+ ion, Figure 10 shows the total e-field on these transferred protons while on the hydronium ions at times starting from 1 ps prior to proton transfer at 0 ps, at which time neutralization of the ions occurs according to eq 1b with H** transferring to the OH^- ion. The oxygen on the hydronium ion is labeled O1′ and the e-field in the H** to O1′ direction, labeled H** → O1′, is shown. There is clearly a weaker e-field on H** while on the H_3O^+ ion toward its covalently bonded oxygen, O1′, than the value shown in Figure 1a for the transferring proton on its covalently bonded oxygen in the H_2O molecule prior to transfer at times less than 0 ps. (Note that O1′ in the hydronium ion was O2 in the original auto-dissociation reaction.) The value of ∼6 V/Å shown in Figure 10 is consistent with the post-transfer values (times greater than 0 ps) shown in Figure 1a that depicts the transferred proton on the hydronium ions.

From Figures 1a,b and 10, proton transfer occurs when e-field values for the proton toward its covalently bonded donor oxygen are below ∼6 V/Å and the proton on H_3O^+ starts out near that low value, consistent with the much lower stability of protons on the hydronium ion than those on the water molecule.

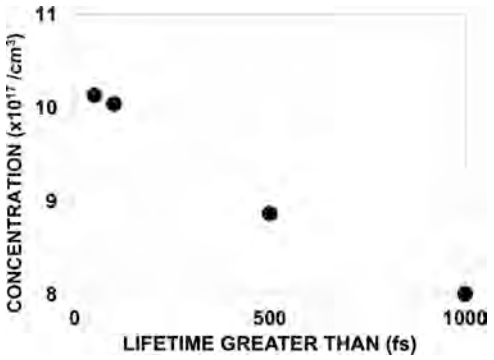

Figure 9. Concentrations of ion pairs as a function of their cumulative lifetimes greater than the abscissa labeled times. From left to right, times are 50, 100, 500, and 1000 fs.

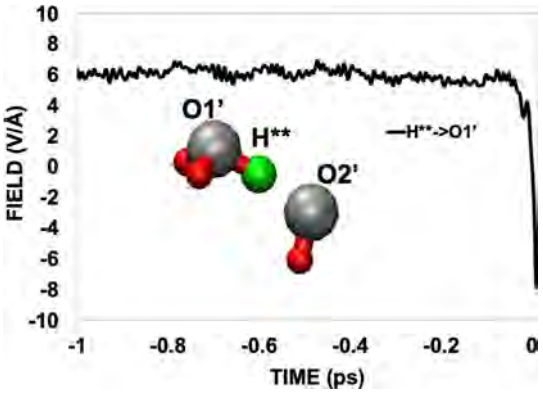

Figure 10. Average local e-field on hydronium proton, H**, in the H** to O1′ direction at times prior to neutralization of the H_3O^+ and OH^- ions that resulted from the original auto-dissociation reaction given in eq 1a. Data averaged over all 20 neutralization reactions.

https://doi.org/10.1021/acs.jpcb.2c06490
J. Phys. Chem. B 2023, 127, 3392−3401

CONCLUSIONS

By using a reactive interatomic potential that matches a variety of scenarios involving water, the current simulations of 27,000 water molecules for 100 ps enable a more complete view of the mechanisms of auto-dissociation of water molecules (where we use the term "auto-dissociation" to mean the initial transfer of a proton from one water molecule to another, without consideration of farther separation of the ions). A result of the simulations is that there is a larger number of auto-dissociations of water molecules than is inferred from dc conductivity studies or equilibrium thermodynamics. Only 20 protons (H*) in 100 ps that were on the donating water oxygen for at least 1 ps show proton transfer via auto-dissociation and remain on the acceptor oxygen for at least 1 ps. Nonetheless, all 20 protons return to their original oxygen donor before the end of the 100 ps analysis period. This is consistent with the rarity of measurable hydronium ions in dc conductivity studies of water that require long-range structural (and vehicular) diffusion away from the reaction site. The data presented here are averaged over those H*.

Volkov et al. propose a concentration of ion pairs (H_3O^+ and OH^-) near 5.4×10^{20} cm^{-3}, or ~2% of the liquid, although they state that their number is an "estimate".[25] Our simulations of the 20 ion pairs detailed in the paper with ion pair lifetimes longer than 1 ps result in a cumulative lifetime concentration (per 100ps runtime) of 8.01×10^{17} cm^{-3} ($1.33x10^{-3}$ mol/L) which is considerably less than the Volkov result but still 2 orders of magnitude higher than that expected from dc conductivity data (10^{-5} vs 10^{-7}). These 20 auto-dissociation events out of 27,000 waters are surprisingly similar to the value of ~10^{-3} auto-dissociation events observed by Ceriotti et al. when they included NQE in their ab initio calculations.[29] The Voronoi volumes around O and H participating in the PT events at the time of transfer are similar to the values observed by Hassanali et al. in their ab initio calculations. These volumes around the H*, O1, and O2 atoms at the time of PT are 10–20% smaller than the average volumes for all other H and O atoms in the system.

The dominant electric field on the transferring proton H* comes from solvent atoms within 6 Å of the proton, with atoms farther away having negligible influence. The value of the local fields averaged over all protons in the system caused by solvent atoms observed here is consistent with the electric fields on water molecules observed in previous simulations that used nonreactive potentials. Use of such potentials could not show the fields at the time of auto-dissociation and the changes that occur as time approached transfer of the proton. Hence, the data presented here provide new insights into the fields from the various contributors within femtoseconds of proton transfer.

Results show that the concomitant hydrogen bond and covalent bond lengths, the acceptor oxygen–donor oxygen–proton (O2–O1–H*) bond angle, O1–O2 spacing, and the electric field induced by solvent atoms on the transferring proton (H*) all change within the last few hundred femtoseconds prior to auto-dissociation in a manner that enhances PT.

The e-field on H* from all atoms within 6 Å of H*, excluding O1 and O2, is shown to be in a direction that enhances PT at 1 ps prior to PT; however, and importantly, this field weakens as time approaches PT. The implication of such a result is that the solvent e-field that excludes the acceptor oxygen O2 helps to orient H* toward O2 but is not a deciding factor in eventual auto-dissociation.

Inclusion of O2 in the calculation of atoms within 6 Å of H* (the intermolecular contribution to the e-field) provides a more complete picture. This intermolecular contribution to the field on H* is strengthened for PT as time approaches PT. This is enhanced by the decrease in O1–O2 distance that lowers the barrier to PT. This provides the definitive evidence of the importance of the acceptor oxygen (O2) on enhancing proton transfer and auto-dissociation caused by the reorientation of the donating molecule and its H* hydrogen bond to O2 and the shortening of the O1–O2 distance. However, once the product ions are formed, our data shows that the e-field on the transferred proton now in the H_3O^+ ion has a weak net e-field to that new covalently bonded O. This weaker field enables an easier transfer of the proton back to the nearby OH^- ion, as evidenced by the neutralization of all ion pairs presented here within the 100 ps run, with an average lifetime of these 20 H_3O^+ ions of 2.5ps.

Even in the case where an angular rotation of the donating water molecule occurs, creating a low O2–O1–H angle, and the e-fields of the solvent molecules are appropriate for PT, the orientation of the acceptor molecule's protons with respect to the potentially transferring proton provides an important factor in the resultant auto-dissociation reaction. Without an appropriate orientation of the accepting water molecule, the transferring proton is unstable as it approaches O2 and can quickly return to O1 in a transient rattle that lasts a few to 10's of femtoseconds. This orientational aspect of the accepting molecule is consistent with data observed in ELF analysis and ab initio calculations showing similar very short-lived transient transfers. Such events are indicative of "rattling" and are different from the case of longer-lived ions presented here.

There are a couple of interrelated criteria that enable auto-dissociation of the water molecule:

(1) a rotation of the donating water molecule to form a more linear, stronger (shorter) hydrogen bond with the accepting oxygen related to the shorter O1–O2 spacing that:

   (a) causes an increase in the covalent bond length that weakens the bond to the donor oxygen[41] and

   (b) also induces a stronger role of the acceptor oxygen (O2) on reducing the e-field in the H* to O1 direction while enhancing it in the H* to O2 direction, thus enhancing auto-dissociation;

(2) a good orientation of the accepting water molecule.

Finally, since the product ions discussed here eventually recombine via eq 1b, results indicate that formation of the structural chains (hydrogen-bonded water wires) that are necessary to separate the ion pairs via proton transfers is less probable, consistent with the low measurable concentrations of such ions in dc conductivity measurements of water. Nonetheless, the unexpectedly large concentration of short-lived ions caused by auto-dissociation of water may offer a potential method for engineering a process involving nano-confined water between 2D layers. Designing a system that gathers these ion products prior to neutralization may offer useful applications.[55,56]

https://doi.org/10.1021/acs.jpcb.2c06490
J. Phys. Chem. B 2023, 127, 3392–3401

■ ASSOCIATED CONTENT

Supporting Information

The Supporting Information is available free of charge at https://pubs.acs.org/doi/10.1021/acs.jpcb.2c06490.

Additional data on individual electric fields and transient transfers (PDF)

■ AUTHOR INFORMATION

Corresponding Author

Stephen H. Garofalini − *Department of Matserials Science and Engineering, Rutgers University, Piscataway, New Jersey 08855, United States;* orcid.org/0000-0003-1718-2034; Email: shg@rutgers.edu

Author

Jesse Lentz − *Department of Matserials Science and Engineering, Rutgers University, Piscataway, New Jersey 08855, United States*

Complete contact information is available at: https://pubs.acs.org/10.1021/acs.jpcb.2c06490

Notes

The authors declare no competing financial interest.

■ ACKNOWLEDGMENTS

The authors acknowledge support from the National Science Foundation (NSF) Environmental Chemical Science Program of the Division of Chemistry, grant number 1609044.

■ REFERENCES

(1) Marx, D.; Tuckerman, M. E.; Hutter, J.; Parrinello, M. The Nature of the Hydrated Excess Proton in Water. *Nature* **1999**, *397*, 601−604.

(2) Markovitch, O.; Chen, H.; Izvekov, S.; Paesani, F.; Voth, G. A.; Agmon, N. Special Pair Dance and Partner Selection: Elementary Steps in Proton Transport in Liquid Water. *J. Phys. Chem. B* **2008**, *112*, 9456−9466.

(3) Woutersen, S.; Bakker, H. J. Ultrafast Vibrational and Structural Dynamics of the Proton in Liquid Water. *Phys. Rev. Lett.* **2006**, *96*, 138305.

(4) Tielrooij, K. J.; Timmer, R. L. A.; Bakker, H. J.; Bonn, M. Structure Dynamics of the Proton in Liquid Water Probed with Terahertz Time-Domain Spectroscopy. *Phys. Rev. Lett.* **2009**, *102*, 198303.

(5) Marx, D.; Chandra, A.; Tuckerman, M. E. Aqueous Basic Solutions: Hydroxide Solvation, Structural Diffusion, and Comparison to the Hydrated Proton. *Chem. Rev.* **2010**, *110*, 2174−2216.

(6) Takahashi, H.; Maruyama, K.; Karino, Y.; Morita, A.; Nakano, M.; Jungwirth, P.; Matubayasi, N. Energetic Origin of Proton Affinity to the Air/Water Interface. *J. Phys. Chem. B* **2011**, *115*, 4745−4751.

(7) Lee, S. H.; Rasaiah, J. C. Proton Transfer and the Mobilities of the H+ and Oh- Ions from Studies of a Dissociating Model for Water. *J. Chem. Phys.* **2011**, *135*, 124505.

(8) Uddin, N.; Kim, J.; Sung, B. J.; Choi, T. H.; Choi, C. H.; Kang, H. Comparative Proton Transfer Efficiencies of Hydronium and Hydroxide in Aqueous Solution: Proton Transfer Vs Brownian Motion. *J. Phys. Chem. B* **2014**, *118*, 13671−13678.

(9) Hassanali, A.; Prakash, M. K.; Eshet, H.; Parrinello, M. On the Recombination of Hydronium and Hydroxide Ions in Water. *Proc. Natl. Acad. Sci. U.S.A.* **2011**, *108*, 20410−20415.

(10) Lockwood, G. K.; Garofalini, S. H. Lifetimes of Excess Protons in Water Using a Dissociative Water Potential. *J. Phys. Chem. B* **2013**, *117*, 4089−4097.

(11) Hassanali, A.; Giberti, F.; Cuny, J.; Kuhne, T. D.; Parrinello, M. Proton Transfer through the Water Gossamer. *Proc. Natl. Acad. Sci. U.S.A.* **2013**, *110*, 13723−13728.

(12) Giberti, F.; Hassanali, A. The excess proton at the air-water interface: The role of instantaneous liquid interfaces. *J. Chem. Phys.* **2017**, *146*, 244703.

(13) Zeng, Y.; Li, A.; Yan, T. Hydrogen Bond Dynamics in the Solvation Shell on Proton Transfer in Aqueous Solution. *J. Phys. Chem. B* **2020**, *124*, 1817−1823.

(14) Headrick, J. M.; Diken, E. G.; Walters, R. S.; Hammer, N. I.; Christie, R. A.; Cui, J.; Myshakin, E. M.; Duncan, M. A.; Johnson, M. A.; Jordan, K. D. Spectral Signatures of Hydrated Proton Vibrations in Water Clusters. *Science* **2005**, *308*, 1765−1769.

(15) Agmon, N.; Bakker, H. J.; Campen, R. K.; Henchman, R. H.; Pohl, P.; Roke, S.; Thämer, M.; Hassanali, A. Protons and Hydroxide Ions in Aqueous Systems. *Chem. Rev.* **2016**, *116*, 7642−7672.

(16) Bandura, A. V.; Lvov, S. N. The Ionization Constant of Water over Wide Ranges of Temperature and Density. *J. Phys. Chem. Ref. Data* **2006**, *35*, 15−30.

(17) Hamann, S. D. The Ionization of Water at High Pressures. *J. Phys. Chem.* **1963**, *67*, 2233−2235.

(18) Chase, M. W.; Curnutt, J. L.; Downey, J. R.; McDonald, R. A.; Syverud, A. N.; Valenzuela, E. A. Janaf Thermochemical Tables, 1982, Supplement. *J. Phys. Chem. Ref. Data* **1982**, *11*, 695−940.

(19) Trout, B. L.; Parrinello, M. Analysis of the Dissociation of H2o in Water Using First-Principles Molecular Dynamics. *J. Phys. Chem. B* **1999**, *103*, 7340−7345.

(20) Sprik, M. Computation of the Pk of Liquid Water Using Coordination Constraints. *Chem. Phys.* **2000**, *258*, 139−150.

(21) Moqadam, M.; Lervik, A.; Riccardi, E.; Venkatraman, V.; Alsberg, B. K.; van Erp, T. S. Local Initiation Conditions for Water Autoionization. *Proc. Natl. Acad. Sci. U.S.A.* **2018**, *115*, E4569−E4576.

(22) Geissler, P. L.; Dellago, C.; Chandler, D.; Hutter, J.; Parrinello, M. Autoionization in Liquid Water. *Science* **2001**, *291*, 2121−2124.

(23) Munoz-Santiburcio, D.; Marx, D. Nanoconfinement in Slit Pores Enhances Water Self-Dissociation. *Phys. Rev. Lett.* **2017**, *119*, 056002.

(24) Wang, R.; Carnevale, V.; Klein, M. L.; Borguet, E. First-Principles Calculation of Water Pka Using the Newly Developed Scan Functional. *J. Phys. Chem. Lett.* **2020**, *11*, 54−59.

(25) Volkov, A. A.; Artemov, V.; Pronin, A. V. A Radically New Suggestion About the Electrodynamics of Water:Can the Ph Index and the Debye Relaxation Be of a Common Origin? *Europhys. Lett.* **2014**, *106*, 46004.

(26) Volkov, A. A.; Artemov, V.; Pronin, A. V. On the Origin of Dielectric Properties of Water. *Dokl. Phys.* **2014**, *59*, 111−114.

(27) Artemov, V. G.; Uykur, E.; Roh, S.; Pronin, A. V.; Ouerdane, H.; Dressel, M. Revealing Excess Protons in the Infrared Spectrum of Liquid Water. *Sci. Rep.* **2020**, *10*, 11320.

(28) Artemov, V. *The Electrodynamics of Water and Ice*; Springer Nature: Switzerland, 2021; Vol. *124*, p 219.

(29) Ceriotti, M.; Cuny, J.; Parrinello, M.; Manolopoulos, D. E. Nuclear Quantum Effects and Hydrogen Bond Fluctuations in Water. *Proc. Natl. Acad. Sci. U.S.A.* **2013**, *110*, 15591−15596.

(30) Chandler, D.; Dellago, C.; Geissler, P. L. Wired-up Water. *Nat. Chem.* **2012**, *4*, 245−247.

(31) Bai, C.; Herzfeld, J. Special Pairs Are Decisive in the Autoionization and Recombination of Water. *J. Phys. Chem. B* **2017**, *121*, 4213−4219.

(32) Marx, D. Proton Transfer 200 Years after Von Grotthuss: Insights from Ab Initio Simulations. *ChemPhysChem* **2006**, *7*, 1848−1870.

(33) Mahadevan, T. S.; Garofalini, S. H. Dissociative Chemisorption of Water onto Silica Surfaces and Formation of Hydronium Ions. *J. Phys. Chem. C* **2008**, *112*, 1507−1515.

(34) Lentz, J.; Garofalini, S. H. Role of the Hydrogen Bond Lifetimes and Rotations at the Water/Amorphous Silica Interface on Proton Transport. *Phys. Chem. Chem. Phys.* **2019**, *21*, 12265−12278.

(35) Reischl, B.; Kofinger, J.; Dellago, C. The Statistics of Electric Field Fluctuations in Liquid Water. *Mol. Phys.* **2009**, *107*, 495−502.
(36) Smith, J. D.; Cappa, C. D.; Wilson, K. R.; Cohen, R. C.; Geissler, P. L.; Saykally, R. J. Unified Description of Temperature-Dependent Hydrogen-Bond Rearrangements in Liquid Water. *Proc. Natl. Acad. Sci.* **2005**, *102*, 14171−14174.
(37) Eaves, J. D.; Loparo, J. J.; Fecko, C. J.; Roberts, S. T.; Tokmakoff, A.; Geissler, P. L. Hydrogen Bonds in Liquid Water Are Broken Only Fleetingly. *Proc. Natl. Acad. Sci. U.S.A.* **2005**, *102*, 13019−13022.
(38) Fecko, C. J.; Eaves, J. D.; Loparo, J. J.; Tokmakoff, A.; Geissler, P. L. Ultrafast Hydrogen-Bond Dynamics in the Infrared Spectroscopy of Water. *Science* **2003**, *301*, 1698−1702.
(39) Hermansson, K.; Ojamäe, L. On the role of electric fields for proton transfer in water. *Solid State Ionics* **1995**, *77*, 34−42.
(40) Saitta, A. M.; Saija, F.; Giaquinta, P. V. Ab-Initio Molecular Dynamics Study of Dissociation of Water under an Electric Field. *Phys. Rev. Lett.* **2012**, *108*, 207801.
(41) Lentz, J.; Garofalini, S. H. Structural Aspects of the Topological Model of the Hydrogen Bond in Water on Auto-Dissociation Via Proton Transfer. *Phys. Chem. Chem. Phys.* **2018**, *20*, 16414−16427.
(42) Mahadevan, T. S.; Garofalini, S. H. Dissociative Water Potential for Molecular Dynamics Simulations. *J. Phys. Chem. B* **2007**, *111*, 8919−8927.
(43) Lockwood, G. K.; Garofalini, S. H. Proton Dynamics at the Water-Silica Interface Via Dissociative Molecular Dynamics. *J. Phys. Chem. C* **2014**, *118*, 29750−29759.
(44) Marx, D.; Tuckerman, M. E.; Parrinello, M. Solvated Excess Protons in Water: Quantum Effects on the Hydration Structure. *J. Phys.: Condens. Matter* **2000**, *12*, A153−A159.
(45) Ma, Y.; Foster, A. S.; Nieminen, R. M. Reactions and Clustering of Water with Silica Surface. *J. Chem. Phys.* **2005**, *122*, 144709.
(46) Kagan, M.; Lockwood, G. K.; Garofalini, S. H. Reactive Simulations of the Activation Barrier to Dissolution of Amorphous Silica in Water. *Phys. Chem. Chem. Phys.* **2014**, *16*, 9294−9301.
(47) Garofalini, S. H.; Mahadevan, T. S.; Xu, S.; Scherer, G. W. Molecular Mechanisms Causing Anomalously High Thermal Expansion of Nanoconfined Water. *ChemPhysChem* **2008**, *9*, 1997−2001.
(48) Xu, S.; Scherer, G. W.; Mahadevan, T. S.; Garofalini, S. H. Thermal Expansion of Confined Water. *Langmuir* **2009**, *25*, 5076−5083.
(49) Xu, S.; Simmons, G. C.; Mahadevan, T. S.; Scherer, G. W.; Garofalini, S. H.; Pacheco, C. Transport of Water in Small Pores. *Langmuir* **2009**, *25*, 5084−5090.
(50) Chandra, A.; Tuckerman, M. E.; Marx, D. Connecting Solvation Shell Structure to Proton Transport Kinetics in Hydrogen−Bonded Networks Via Population Correlation Functions. *Phys. Rev. Lett.* **2007**, *99*, 145901.
(51) Chen, H.; Voth, G. A.; Agmon, N. Kinetics of Proton Migration in Liquid Water. *J. Phys. Chem. B* **2010**, *114*, 333−339.
(52) Tuckerman, M. E.; Chandra, A.; Marx, D. A Statistical Mechanical Theory of Proton Transport Kinetics in Hydrogen-Bonded Networks Based on Population Correlation Functions with Applications to Acids and Bases. *J. Chem. Phys.* **2010**, *133*, 124108.
(53) Tuckerman, M. E.; Marx, D.; Klein, M. L.; Parrinello, M. On the Quantum Nature of the Shared Proton in Hydrogen Bonds. *Science* **1997**, *275*, 817−820.
(54) Hassanali, A.; Giberti, F.; Sosso, G. C.; Parrinello, M. The Role of the Umbrella Inversion Mode in Proton Diffusion. *Chem. Phys. Lett.* **2014**, *599*, 133−138.
(55) Xu, J.; Jiang, H.; Shen, Y.; Li, X.-Z.; Wang, E. G.; Meng, S. Transparent Proton Transport through a Two Dimensional Nanomesh Material. *Nat. Commun.* **2019**, *10*, 3971.
(56) Feng, Y.; Chen, J.; Fang, W.; Wang, E. G.; Michaelides, A.; Li, X. Z. Hydrogenation Facilitates Proton Transfer through Two-Dimensional Honeycomb Crystals. *J. Phys. Chem. Lett.* **2017**, *8*, 6009−6014.

https://doi.org/10.1021/acs.jpcb.2c06490
J. Phys. Chem. B 2023, 127, 3392−3401